High-temperature carrier transport and thermoelectric properties of heavily La- or Nb-doped $SrTiO_3$ single crystals

Shingo Ohta and Takashi Nomura
Nagoya University, Graduate School of Engineering, Nagoya 464-8603, Japan

Hiromichi Ohta and Kunihito Koumoto[a)]
Nagoya University, Graduate School of Engineering, Nagoya 464-8603, Japan and CREST, Japan Science and Technology Agency, Kawaguchi 332-0012, Japan

(Received 6 July 2004; accepted 12 November 2004; published online 5 January 2005)

Electron and thermal transport properties, i.e., electrical conductivity, carrier concentration, Hall mobility, Seebeck coefficient, thermal conductivity, of heavily La- or Nb-doped $SrTiO_3$ (STO) bulk single crystals were measured at high temperatures, (300–1050 K) to clarify the influence of doping upon the thermoelectric performance of STO. The temperature dependence of Hall mobility and Seebeck coefficient changed at ~750 K in all samples because the dominant mechanism for carrier scattering changed with increasing temperature from coupled scattering by polar optical phonons and acoustic phonons to mere acoustic phonon scattering. The density-of-states effective mass of Nb-doped STO, which was estimated from the carrier concentration and Seebeck coefficient, was larger than that of La-doped STO. Thermal conductivity of the samples, which was similar to that of undoped STO single crystal, decreased proportionally to T^{-1}, indicating that the phonon conduction takes place predominantly and the electronic contribution to thermal conductivity is negligible. © *2005 American Institute of Physics*. [DOI: 10.1063/1.1847723]

INTRODUCTION

Thermoelectric semiconductors such as SiGe and Bi_2Te_3 are applied to power generators and refrigerators utilizing Seebeck and Peltier effect, respectively.[1] The energy conversion performance of thermoelectric semiconductors is usually evaluated by using the dimensionless figure of merit, $ZT=S^2\sigma/\kappa$, where Z, T, S, σ, and κ are the figure of merit, absolute temperature, Seebeck coefficient, electrical conductivity, and thermal conductivity, respectively. Practical applications generally require $ZT \geqslant 1$. Only a few intermetallic compound semiconductors such as Bi_2Te_3 alloys,[2] $AgPb_{18}SbTe_{20}$,[3] and filled skutterudite antimonides[4] are known to fulfill the requirement to date. Although the major thermoelectric materials had been intermetallic compound semiconductors, Na_xCoO_2 was found in 1997 to show high thermoelectric performance[5] and thermoelectric oxides have drawn great attention and interest since then.

Na_xCoO_2 exhibits a large power factor (PF), 5×10^{-3} W m^{-1} K^{-2}, which is comparable to that of practical Bi_2Te_3, due to rather large carrier effective mass (m^*), which reflects the large Seebeck coefficient, of Na_xCoO_2. Hence, oxide semiconductors having heavy carriers are expected to be promising candidates for high-performance thermoelectric materials.

Heavily electron-doped $SrTiO_3$ (STO) is considered to be an appropriate n-type oxide semiconductor for high-temperature thermoelectric application for the following reasons. First, the m^* of the mobile electrons in STO is two orders of magnitude larger ($\sim 10\ m_0$) than that of conventional thermoelectric semiconductors ($\sim 0.1\ m_0$).[6] Second, carrier concentration of STO can be easily controlled to be an insulator to degenerate semiconductor ($\sim 10^{21}$ cm^{-3}) by appropriate substitutional doping. Accordingly, the absolute value of Seebeck coefficient of heavily doped STO can be maintained large even when the carrier concentration is very high ($\sim 10^{21}$ cm^{-3}).[7]

Very recently, high-temperature thermoelectric performance of heavily doped ceramic samples of STO has been reported.[8,9] However, the performance is still low as compared to that of p-type oxide semiconductors,[10] because both electronic and thermal transport would be affected by grain boundaries in polycrystalline ceramics. Therefore, the intrinsic thermoelectric performance of STO at high temperatures is still unknown.

We, therefore, measured high-temperature electron transport and thermoelectric properties of heavily La-doped STO (La–STO) or Nb-doped STO (Nb–STO) single crystals to clarify its intrinsic thermoelectric performance at high temperatures. In this study, we focused on the effect of heavy doping of either Nb at the Ti site or La at the Sr site upon the m^*.

EXPERIMENTAL

Bulk single-crystal samples of La–STO or Nb–STO, which had been grown by a conventional Verneuil method at 2080 °C (Earth Chemical Co.[11]), were used in this study. The doping levels of the samples are summarized in Table I. The σ of the samples were measured by dc four probe method using the van der Pauw configuration. The S was measured by a conventional steady state method under Ar atmosphere.[12,13] The κ of the sample was obtained by separate measurements using calorimetry for heat capacity and laser flush for thermal diffusivity under vacuum.

[a)]Author to whom correspondence should be addressed; electronic mail: g44233a@nucc.cc.nagoya-u.ac.jp

TABLE I. Doping levels of the single-crystal samples of La- and Nb-doped $SrTiO_3$.

(a)	(b)	(c)	(d)
La-doped (8.4×10^{19} cm^{-3})	La-doped (8.4×10^{20} cm^{-3})	Nb-doped (1.6×10^{20} cm^{-3})	Nb-doped (3.3×10^{20} cm^{-3})

RESULTS AND DISCUSSION

Electron transport and thermoelectric properties of the La–STO and Nb–STO samples are summarized in Table II. The n of each sample corresponds very well to the doping level. The μ of the La–STO samples is 6–7 cm^2 V^{-1} s^{-1}, while that of the Nb–STO samples is 5–6 cm^2 V^{-1} s^{-1}. The S is negative in all cases indicating n-type semiconductivity. The κ of both the La–STO and Nb–STO was $\sim$12 W m^{-1} K^{-1} comparable to that of undoped-STO.[14]

Figure 1 shows the temperature dependence of S for La–STO and Nb–STO. The absolute value of S increased with an increase in temperature in all cases due to an increase in the Fermi integral with temperature. An anomaly of the Seebeck coefficient is clearly observed at $\sim$750 K in all cases. The reason for this phenomenon can be understood as follows. The S of an n-type semiconductor can be expressed by the following equation as reported by Vining:[15]

$$S = -\frac{k_B}{e}\left(\frac{(r+2)F_{r+1}(\xi)}{(r+1)F_r(\xi)} - \xi\right), \tag{1}$$

where k_B, ξ, r, and F_r are the Boltzmann constant, chemical potential, scattering parameter of relaxation time, and Fermi integral, respectively. The F_r is given by

$$F_r(\xi) = \int_0^\infty \frac{x^r}{1+e^{x-\xi}}dx. \tag{2}$$

The n is given by

$$n_- = 4\pi\left(\frac{2m^* k_B T}{h^2}\right)^{3/2} F_{1/2}(\xi), \tag{3}$$

where h, T, and m^* are the Planck constant, absolute temperature, and density-of-states effective mass, respectively. Above $\sim$750 K, carriers are scattered only by acoustic phonons and the scattering parameter of relaxation time is $r=0$.[16] In contrast, below $\sim$750 K, carriers are scattered by both polar optical phonons and acoustic phonons, and the scattering parameter of relaxation time gradually increases with decreasing temperature reaching 0.5 at room temperature (polar optical phonon scattering) as shown in Fig. 1. The m^* values of the La–STO and Nb–STO, which were estimated using the n and S, are also shown in Fig. 1. The m^* of the Nb–STO ($m^*=7.3$–$7.7\ m_0$) is larger than that of La–STO ($m^*=6.0$–$6.6\ m_0$).

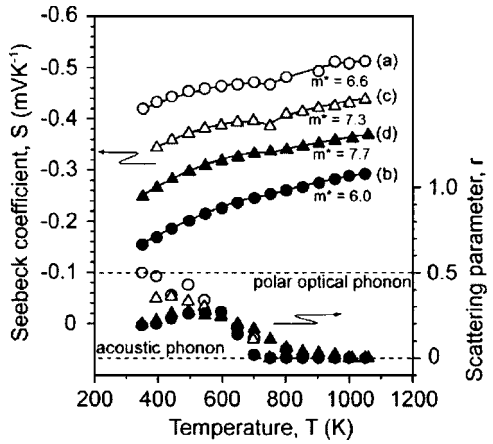

FIG. 1. Temperature dependence of Seebeck coefficient, S, for (a) La-doped (8.4×10^{19} cm^{-3}), (b) La-doped (7.9×10^{20} cm^{-3}), (c) Nb-doped (1.6×10^{20} cm^{-3}), and (d) Nb-doped (3.3×10^{20} cm^{-3}) $SrTiO_3$ bulk single crystals. Temperature dependencies of carrier scattering factor, r, calculated from the measured data are also shown.

Figure 2 shows the temperature dependence of σ for La–STO and Nb–STO. The σ decreases proportionally to $T^{-2.0}$ below $\sim$750 K and $T^{-1.5}$ above $\sim$750 K. The temperature dependencies of n and μ are also shown in the inset. Although n did not show any significant temperature dependence, μ decreased proportionally to $T^{-2.0}$ below $\sim$750 K and $T^{-1.5}$ above $\sim$750 K, most likely because the dominant mechanism of carrier scattering changed with increasing temperature from coupled scattering by polar optical phonons together with acoustic phonons to mere acoustic phonon scattering.

Figure 3 shows the temperature dependence of κ for La–STO and Nb–STO. The κ decreased proportionally to T^{-1}, indicating that the thermal transport is dominated by phonon conduction. In fact the κ due to the electron contribution (κ_{el}) was $\sim$0.5 W m^{-1} K^{-1}, which was estimated using the Wiedemann–Franz law. Although the κ_{el} increases with in-

TABLE II. Electrical conductivity (σ), carrier concentration (n), Hall mobility (μ), Seebeck coefficient (S), power factor ($S^2\sigma$), thermal conductivity (κ), and figure of merit (Z,ZT) for La- and Nb-doped $SrTiO_3$ measured at room temperature.

	STO	σ (S cm^{-1})	n (10^{20} cm^{-3})	μ (cm^2 V^{-1} s^{-1})	S (mV K^{-1})	$S^2\sigma$ (10^{-4} W m^{-1} K^{-2})	κ (W m^{-1} K^{-2})	Z (10^{-5} K^{-1})	ZT (–)
(a)	La-doped (8.4×10^{19} cm^{-3})	54	0.5	7.0	−0.42	9.5	12	7.9	0.02
(b)	La-doped (8.4×10^{20} cm^{-3})	1000	6.8	9.2	−0.15	23	9.1	25	0.08
(c)	Nb-doped (1.6×10^{20} cm^{-3})	95	1.5	6.2	−0.33	10	11	9.3	0.03
(d)	Nb-doped (3.3×10^{20} cm^{-3})	353	3.7	6.0	−0.24	20	9.6	21	0.06

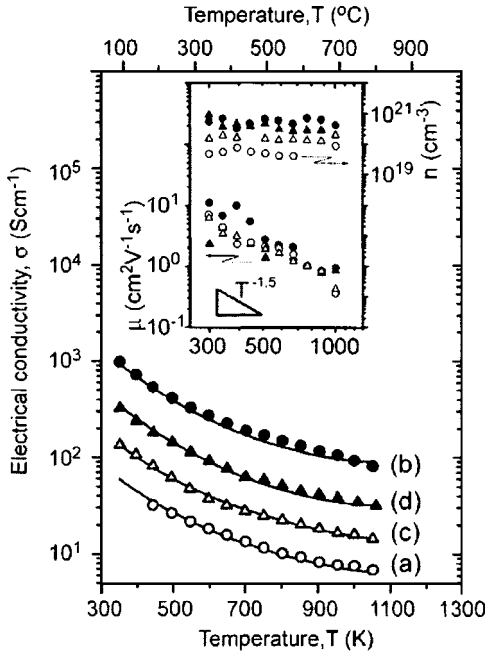

FIG. 2. Temperature dependence of electrical conductivity, σ, for (a) La-doped (8.4×10^{19} cm^{-3}), (b) La-doped (7.9×10^{20} cm^{-3}), (c) Nb-doped (1.6×10^{20} cm^{-3}), and (d) Nb-doped (3.3×10^{20} cm^{-3}) $SrTiO_3$ bulk single crystals. Hall mobility, μ, and carrier concentration, n, of the single-crystal samples are also shown in the inset.

creasing n, the κ_{total} shows no significant dependence on the n because the contribution of $\kappa_{lattice}$ is dominant.

Figure 4 shows the temperature dependence of the Z for La–STO and Nb–STO. The ZT at room temperature of La–STO is ~0.03, which is the largest value so far reported for n-type oxide semiconductors. The absolute value of the S decreases above ~750 K, which leads to a slight decrease in the Z with increasing temperature, in spite of the decrease in

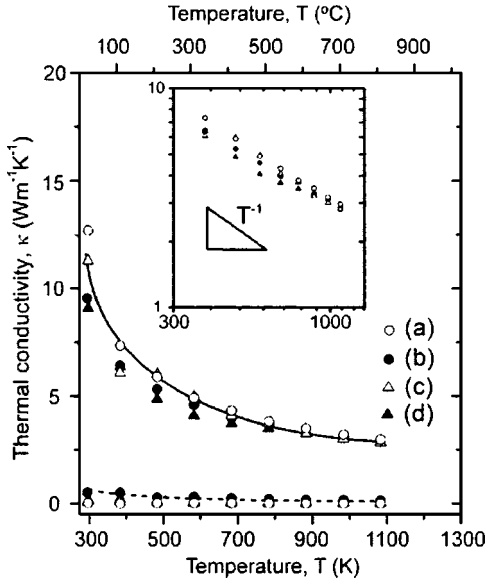

FIG. 3. Temperature dependence of thermal conductivity, κ, for (a) La-doped (8.4×10^{19} cm^{-3}), (b) La-doped (7.9×10^{20} cm^{-3}), (c) Nb-doped (1.6×10^{20} cm^{-3}), and (d) Nb-doped (3.3×10^{20} cm^{-3}) $SrTiO_3$ bulk single crystals. Solid lines indicate total thermal conductivity and dotted lines indicate electronic thermal conductivity (κ_{el}) estimated using the Wiedemann–Franz law. The κ decreasing proportionaly to T^{-1} is shown in the inset.

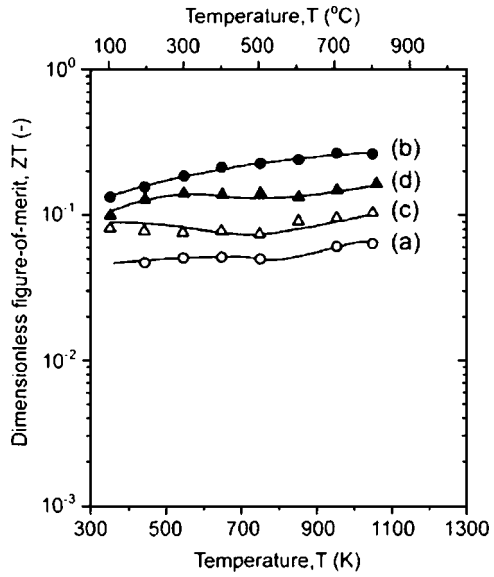

FIG. 4. Dimensionless thermoelectric figure-of-merit, ZT, for (a) La-doped (8.4×10^{19} cm^{-3}), (b) La-doped (7.9×10^{20} cm^{-3}), (c) Nb-doped (1.6×10^{20} cm^{-3}), and (d) Nb-doped (3.3×10^{20} cm^{-3}) $SrTiO_3$ bulk single crystals.

κ with increasing temperature. It should be noted that the Z of both La–STO and Nb–STO increased with increasing carrier concentration and the largest ZT of 0.27 at 1073 K was attained in La-[8.4×10^{20} cm^{-3}] doped STO which has the largest carrier concentration in all samples. This observation is consistent with our view that heavily doped degenerate semiconductors with large m^* of carriers should demonstrate high thermoelectric performance.

SUMMARY

We clarified herein intrinsic thermoelectric performance of heavily La- and Nb-doped $SrTiO_3$ bulk single crystals and effect of La- and Nb-doping upon carrier effective mass (m^*). The temperature dependence of μ and S changed at ~750 K in all samples, indicating that the dominant carrier scattering mechanism changes with increasing temperature from a coupled scattering by polar optical phonons and acoustic phonons to mere acoustic phonon scattering. The κ of the samples, which was similar to that of undoped $SrTiO_3$ single crystal at room temperature, decreased proportionally to T^{-1}, indicating that the lattice thermal conduction occurs predominantly. The m^* of the Nb-doped STO ($m^*=7.3-7.7\ m_0$) is larger than that of La-doped STO ($m^*=6.0-6.6\ m_0$).

ACKNOWLEDGMENTS

The authors would like to thank Tsubaki of Earth Chemical Co. for giving La-, Nb- single-crystal $SrTiO_3$ plates. The authors would also like to thank Dr. W. Wunderlich (CREST, JST) for carefully reading the manuscript.

[1]G. Mahan, B. Sales, and J. Sharp, Phys. Today **50**, 42 (1997).
[2]T. Caillat, M. Carle, P. Pierrat, H. Scherrer, and S. Scherrer, J. Phys. Chem. Solids **53**, 1121 (1992).
[3]K. F. Hsu, S. Loo, F. Guo, W. Chen, J. S. Dyck, C. Uher, T. Hogan, E. K. Polychroniadis, and M. G. Kanatzidis, Science **303**, 818 (2004).

[4]B. C. Sales, D. Mandrus, B. C. Chakoumakos, V. Keppens, and J. R. Thompson, Phys. Rev. B **56**, 15081 (1997).
[5]I. Terasaki, Y. Sasago, and K. Uchinokura, Phys. Rev. B **56**, 12685 (1997).
[6]T. Caillat, A. Borshchevsky, and J. P. Fleurial, J. Appl. Phys. **80**, 4442 (1996).
[7]T. Okuda, K. Nakanishi, S. Miyasaka, and Y. Tokura, Phys. Rev. B **63**, 113104 (2001).
[8]H. Muta, K. Kurosaki, and S. Yamanaka, J. Alloys Compd. **350**, 292 (2003).
[9]H. Muta, K. Kurosaki, and S. Yamanaka, J. Alloys Compd. **368**, 22 (2004).
[10]K. Fujita, T. Mochida, and K. Nakamura, Jpn. J. Appl. Phys., Part 1 **40**, 4644 (2001).
[11]http://www.furuchi.co.jp/JAPEN/history.htm
[12]D. Olaya, F. Pan, C. T. Rogers, and J. C. Price, Appl. Phys. Lett. **80**, 2928 (2002).
[13]We measured the diffuse reflectance spectra ($\lambda = 200-2500$ nm) to investigate thermal stability of Nb-doped $SrTiO_3$ powder in air and Ar atmosphere. We found that the carrier concentration stayed almost constant in Ar atmosphere up to 800 °C (see Fig. 1), but it decreased above ~400 °C in air.
[14]A. J. Sievers, Bull. Am. Phys. Soc. **8**, 208 (1963).
[15]C. B. Vining, J. Appl. Phys. **69**, 331 (1991).
[16]K. Durczewski and M. Ausloos, Phys. Rev. B **61**, 5303 (2000).